Capsicumine: a new peptide from red peppers turns out to be a powerful antibiofilm agent and displays a new mechanism of action, matrix anti-assembly

Rafael Gomes Von Borowski[1,2], Sophie Chat[1], Rafael Schneider[1,2], Emmanuel Giudice[1], Aline Rigon Zimmer[2], Simone Cristina Baggio Gnoatto[2], Alexandre José Macedo[2,3,*], and Reynald Gillet[1,*]

[1] Univ. Rennes, CNRS, Institut de Génétique et Développement de Rennes (IGDR) UMR 6290, Rennes, France, France; [2]Programa de Pós-Graduação em Ciências Farmacêuticas, Faculdade de Farmácia, Universidade Federal do Rio Grande do Sul, 90610-000 Porto Alegre, Brazil; and [3]Centro de Biotecnologia da Universidade Federal do Rio Grande do Sul, 91501-970 Porto Alegre, Brazil

[*]To whom correspondence may be addressed. Email reynald.gillet@univ-rennes1.fr or alexandre.jose.macedo@gmail.com.

Abstract

Biofilm-forming bacteria are an important reservoir of nosocomial infections, and source of antibiotic resistance and tolerance. These bacteria are enclosed in a complex matrix that allows them to adhere to medical devices and tissue, and which also protects against antibiotics and immune systems. Advances in antibiofilm strategies for targeting the biofilm matrix are therefore extremely relevant in the fight against multidrug-resistant and/or -tolerant bacteria. Plants are constantly attacked by a wide range of pathogens, and have protective factors such as peptides to defend themselves. These peptides are common components in *Capsicum* red pepper seeds, and here we investigate and identify a new antibiofilm peptide, "capsicumicine." We demonstrate that capsicumicine prevents methicillin-resistant *Staphylococcus epidermidis* adhesion as well as biofilm establishment and maintenance via a new extracellular "matrix anti-assembly" (MAA) mechanism of action. In this manner, capsicumicine disturbs the construction of the matrix, and therefore its functioning. Importantly, the peptide is not an antibiotic and it is not cytotoxic, thus capsicumicine is an exciting new alternative treatment for prevention of biofilm infections.

Keywords: antibiofilm, biofilm, matrix, peptides, matrix anti-assembly, resistance, tolerance.

Significance

Both pathogenic drug resistance and tolerance are favored by biofilm development. Indeed, biofilm-covered microorganisms display antibiotic resistance up to 1000 times higher than planktonic ones. *Staphylococcus epidermidis* is remarkably good at forming biofilm, and is therefore highly associated with medical device infection. Here, we report the discovery of "capsicumicine," a novel antibiofilm peptide derived from *Capsicum bacattum*. This prevents the establishment of *S. epidermidis* biofilm via a new mechanism of action, matrix anti-assembly (MAA). MAA is not antibiotic, and is based on extracellular interactions that force bacteria to remain planktonic, letting immune systems and

traditional antibiotics more easily clear the infection. For this reason, MAA should confer a lower susceptibility to bacterial resistance development. Very importantly, capsicumicine is not cytotoxic.

Introduction

Antimicrobial failure is a worldwide challenge, currently addressed by a WHO global action plan (*1*). A lack of new antibiotics and the inappropriate use of older treatments mean that multidrug-resistant strains are increasing (*2*). This process is favored by biofilm development, and microorganisms enclosed in biofilm matrix have antibiotic resistance that is up to 1000 times higher than planktonic ones (*3-5*). This makes the matrix itself an important target for biofilm control. Biofilms are organized microbial clusters made of a self-assembled matrix that usually attaches to a surface, whether abiotic (medical devices, teeth, etc.) or biotic (host tissues, mucus, inside chronic wounds, etc.) (*6, 7*). Since the bacteria are embedded into this self-assembled matrix, they are harder to treat because of their increased tolerance and resistance to antibiotics, disinfectants, and host defenses (*8, 9*). Other advantages over planktonic forms include physiological and biochemical changes, beneficial quorum sensing, higher (up to 100 times) mutation rates, and persister cell development (*10-14*). Therefore, the development of antivirulence strategies such as efficient antibiofilm agents is crucial for the current antibiotic crisis, and peptides and peptidomimetics are an increasingly important arsenal for controlling pathogenic biofilms (*15-19*).

Staphylococcus epidermidis is the most frequent coagulase-negative staphylococcal (CoNS) infection-causing disease (*20, 21*), surviving on various surfaces for months (*22, 23*). It is present in 30% of health care-involving bloodstream infections, and is significantly associated with medical device infections, including 15-40% of prosthetic valve endocarditis (*24, 25*) and 30-43% of prosthetic orthopedic device infections (*26-28*). More than 150 million intravascular catheters are used per year in the USA, and there are about 250,000 catheter-related infections (*29-31*). *S. epidermidis* is developing antibiotic multi-resistances such as elevated glycopeptide minimal inhibitory concentrations (*32-34*), and 73-88% of isolates display resistance to oxacillin, fluoroquinolones, macrolides, clindamycin, and trimethoprim/sulfamethoxazole (*35-37*). While *S. epidermidis* expresses many virulence factors such as toxins, proteases, enzymes, surface and extracellular proteins, and capsules (*38*), the formation of biofilm is the most important mechanism in infection development (*23, 28*). The extracellular matrix is a complex physicochemical barrier and thus represents one of the biggest challenges in biofilm treatment (*6*).

Here, we report the discovery of a novel antibiofilm peptide, capsicumicine, derived from the seeds of the red pepper *Capsicum baccatum.* It prevents methicillin-resistant *S. epidermidis* adhesion, as well as biofilm establishment and maintenance. Notably, we show that capsicumicine's antibiofilm activity is due to a new extracellular mechanism of action, matrix anti-assembly (MAA). Since capsicumicine is non-antibiotic and non-cytotoxic, it provides an exciting new alternative in the fight against biofilm infections.

Results

Capsicumicine prevents biofilm formation without antibiotic activity. To begin, we commercially synthesized three peptides of a natural fraction derived from *Capsicum baccatum* var. *pendulum* pepper seeds. P1 (RVQSEEGEDQISQRE), P2 (RAEAFQTAQALPGLCRI), and P3 (RSCQQQIQQAQQLSSCQQYLKQ) were the most stable fragments after chromatographic purification,

enzymatic digestion and MALDI-MS fragmentation. To find the most active one, we exposed these compounds to strong biofilm-forming *S. epidermidis* RP62A (ATCC 35984). After 24 h, crystal violet was used to quantify the remaining biofilm, and P3, "capsicumicine," was the most active, with particularly strong antibiofilm activity. Biofilm decreases were observed at all tested concentrations, but especially at 10 µM. There, biofilm was reduced by over 91%, independently of cell growth inhibition and not dependent on dose-response (Fig. 1*A*). To examine the effects of capsicumicine on growth, we checked *S. epidermidis* colony-forming unit (CFU) counts after peptide exposure. As expected, the CFUs were unchanged by capsicumicine, so the peptide's biofilm inhibition is not due to bactericidal activity (Fig. 1*B*). In order to localize the peptide, we used capsicumicine conjugated to fluorescein isothiocyanate (capsicumicine-FITC) and confocal fluorescence microscopy (CFM). Analysis of the CFM images showed that capsicumicine-FITC stays associated with extracellular matrix components, not entering into bacterial cells or the walls or membranes (Fig. 1 *C* and *D*).

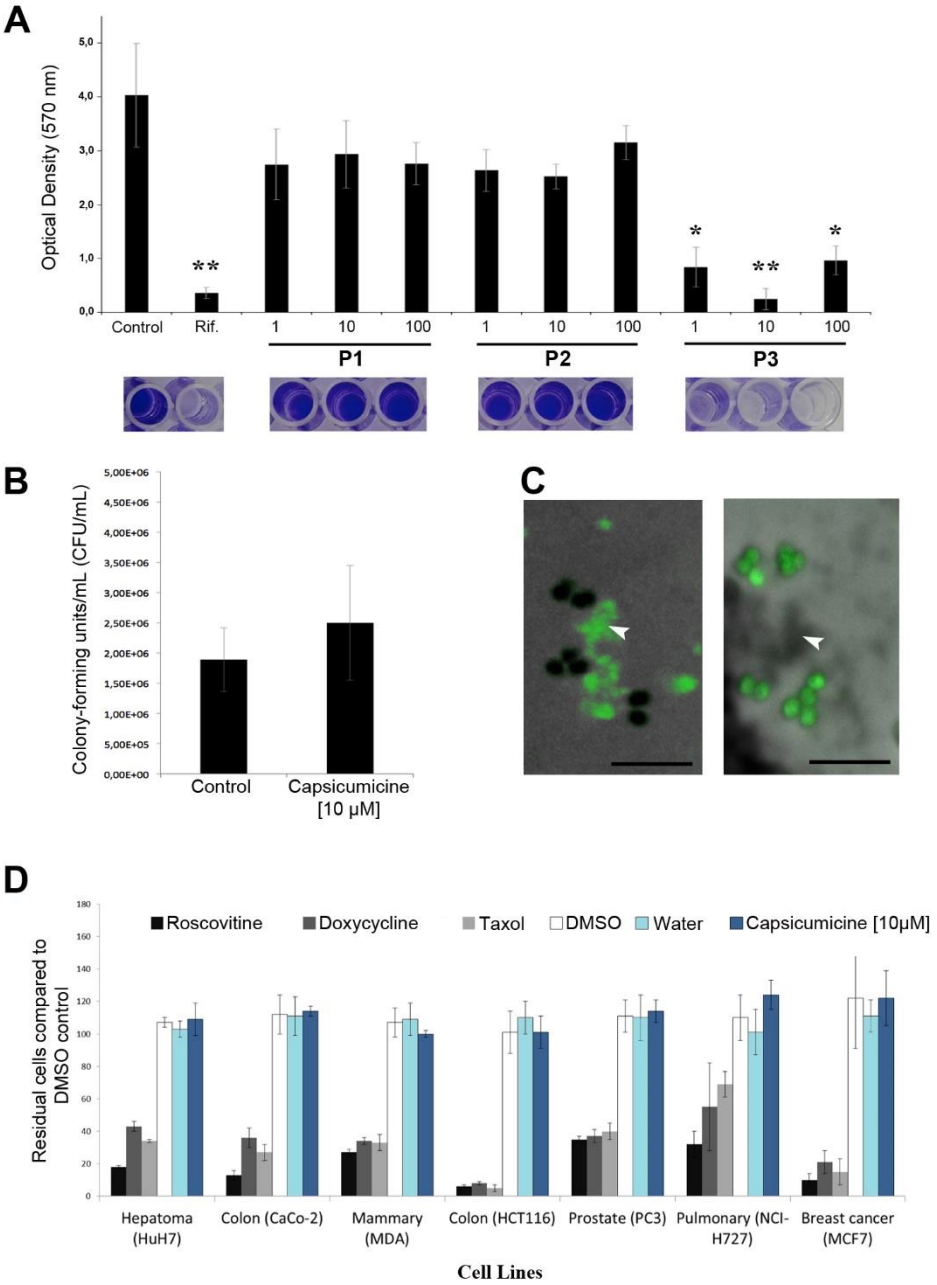

Fig. 1. Antibiofilm activity of 3 peptides. *(A)* Antibiofilm activity of peptides P1, P2, and P3 (capsicumicine) at 1, 10, and 100 µM. Quantification (black bars) of *Staphylococcus epidermidis* (ATCC 35984) biofilms was done at an optical density of 570 nm after 24 h of peptide exposure, and is shown compared to the bacteria without peptide exposure (Control) and the antibiotic control, 16 µg/mL rifampicin (Rif.). Below the graph, photos illustrate the wells after crystal violet treatment. Student's *t*-test: *, $p \leq 0.05$; **, $p \leq 0.01$. *(B)* Colony-forming units (CFUs) after 24 h exposure to 10 µM capsicumicine. Instead of the peptide, the control was exposed to vehicle (water), and the result is shown as CFU/mL. *(C)* Confocal fluorescence microscopy (CFM) images: *(left) S. epidermidis* after exposure to 10 µM capsicumicine fluorescein isothiocyanate (capsicumicine-FITC), with the matrix green (fluorescence), and the bacterial cells black (no fluorescence); and (*right*) control *S. epidermidis*

after exposition to an antibacterial peptide-FITC, this time showing a gray matrix (no fluorescence) and green bacterial cells (fluorescence). White arrows indicate matrix content. Scale bars, 5 µm. *D*) Capsicumicine cytotoxicity evaluation in representative human cell lines shown via automated image-based cellular content analysis. Cell counts are presented as residual cell percentages (%) compared to the average of the DMSO control (white), with water control also shown (light blue). The three bars on the left show cytotoxic controls (roscovitine, doxycycline, and taxol), while the darker blue bars are cells exposed to 10 µM capsicumicine.

Effects of capsicumicine on the eradication of structured biofilms. To verify the interactions between capsicumicine and established matrices, we exposed a pre-existing *S. epidermidis* biofilm to a single concentration (100 µM) of the peptide, then after 24 h used crystal violet to quantify the total biomass. At that concentration, capsicumicine accounts for only about 15% of the disruption of pre-existing biofilm (Fig. S1).

Capsicumicine is not cytotoxic in mammalian cells. To ensure that capsicumicine is safe, we verified its biological cytotoxicity in seven different representative human cell lines. We used automated image-based cellular content analysis, and found that capsicumicine-treated cells perform exactly the same as untreated controls, thus there is no cytotoxicity (Fig. 1*E*).

Independently of cell interactions, capsicumicine impairs initial biofilm attachment, aggregation, and accumulation. To explore its activity during the first stages of biofilm development, we analyzed biofilm cultures on polystyrene coupons with and without capsicumicine after 1, 4, and 24 h. Scanning electron microscopy (SEM) analysis shows that bacterial attachment decreases after 1 h of capsicumicine exposure, with biofilm accumulation and cell aggregation profiles strongly reduced after 4 and 24 h (Fig. 2*A*). This demonstrates that capsicumicine prevents *S. epidermidis* coupon adhesion, and notably this activity still occurs after 24 h incubation. To study the peptide's possible mechanisms of action, we selected several genes involved in different stages of biofilm development (*atlE*, *aap*, *agrC*, *icaA*, *leuA*, *saeR*, *saeS,* and *sarA*), with primers listed in Table S1. Fold changes were analyzed by quantitative real-time PCR (qRT-PCR). Since exposed bacteria remain planktonic, we compared their relative gene expressions to planktonic control cells. For all tested genes, capsicumicine-exposed cells show the same fold changes as the control (Fig. 2*B*).

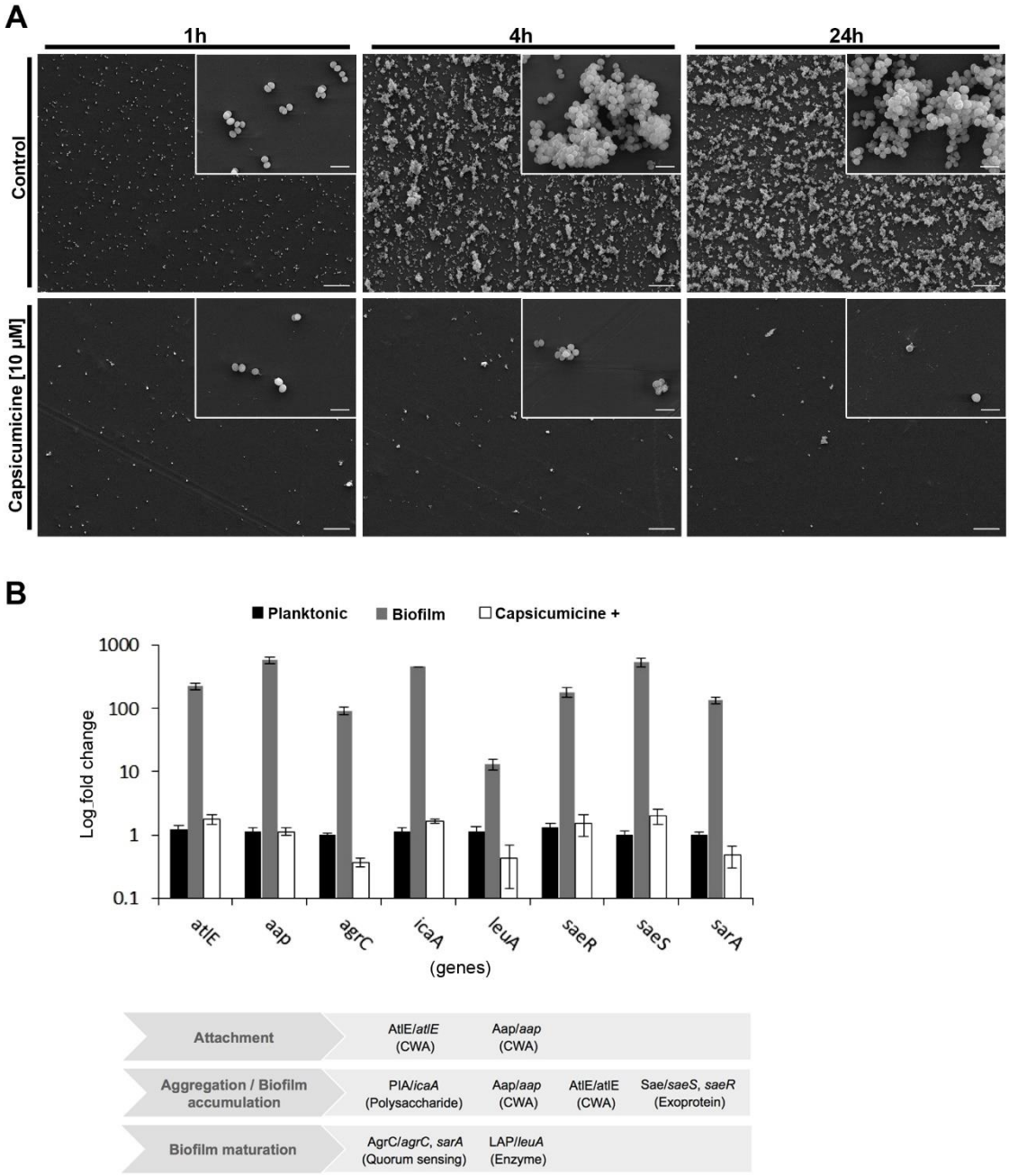

Fig. 2. Scanning electron microscopy (SEM) and qRT-PCR analysis. (*A)* SEM images of polystyrene coupons after 1, 4, or 24h of culture with *Staphylococcus epidermidis* (ATCC 35984). *Top:* peptide-less biofilm control; *bottom:* cultures exposed to 10 µM capsicumicine. Magnification x500, with insets at x5,000; scale bars, 10 µm. (*B*) Gene expression (mean log fold changes ± standard errors of the means) of the encoding genes involved in *S. epidermidis* biofilm formation as compared to the planktonic (black) and biofilm controls (gray), with the *ssrA* gene used as a reference. The group exposed to the peptide (capsicumicine +) are white. CWA, cell wall-anchored proteins.

Capsicumicine disturbs *S. epidermidis* matrix assembly. Since capsicumicine's antibiofilm activity was not associated with direct bacterial interactions or gene expression modulation, we used various microscopic approaches to investigate the interactions between the peptide and the extracellular

matrix. In the biofilm control, macroscopic observation shows a homogenous whitish adhered layer covering the walls and bottoms of the well (Fig. 3*A*, middle), but when capsicumicine is present, we see whitish flocculent non-adhered heterogeneous agglutinates (Fig. 3*A*, right). Transmitted light microscopy images (Fig. 3*B*) match these macroscopic observations. Similarly, CFM images confirm the presence of labelled-capsicumicine in the matrix, which displays a smooth cloud-like appearance (Fig. 3*C*). Crucially, scanning and transmission electron microscopy (SEM and TEM) techniques yield ultra-structural descriptions that support these results, with the control biofilm matrix showing denser assembled globular-like structures, while the capsicumicine-exposed matrix is clearly less dense and has thin fibrillary branch-like structures (Fig. 3 *D* and *E*). Therefore, different imaging techniques prove that matrix assembly changes when capsicumicine is present. Furthermore, since cellular morphologies are not different from the controls, the peptide and bacteria do not seem interact.

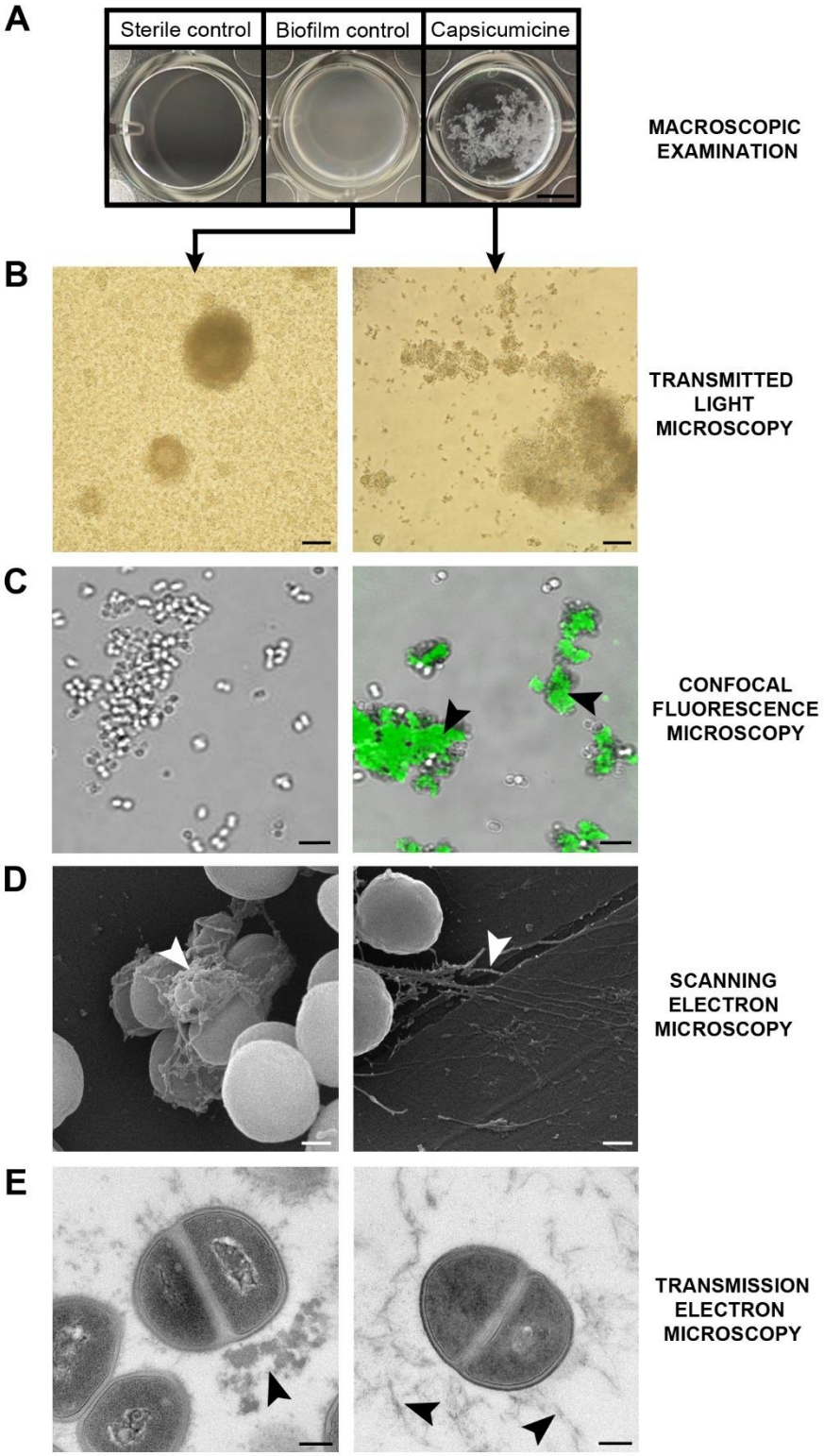

Fig. 3. Different microscopic images of *Staphylococcus epidermidis* (ATCC 35984) biofilm. These images explore the organizational state of the biofilm matrix after 24 h in the presence (*right*) or absence (control, *left*) of capsicumicine. (*A*) Macroscopic examination using pictures from the bottom of 24-well plates. The "sterile control" shows no bacteria or biofilm formation; the "biofilm control" has homogenous adhered layers of bacteria; and "capsicumicine" has non-adhered bacteria which agglutinate in the peptide's presence. (*B*) Transmitted light microscopy images show the biofilm

control has many overlapping attached cells surrounded by a matrix next to bacterial clusters, while the capsicumicine-exposed culture has non-adhered but suspended cells that look to be agglutinated. (*C*) Confocal fluorescence microscopy images of the fluorescence-free control and the capsicumicine-FITC, featuring a green fluorescent matrix. (*D*) Like the previous images, scanning electron microscopy images show the control with dense globular-like matrix features, while the capsicumicine-exposed culture has fibrillary branch-like oligomer structures. (*E*) Transmission electron microscopy images shows denser assembled structures in the biofilm matrix control, while the capsicumicine-exposed matrix is less dense and displays thin fibrillary oligomer structures. Arrows indicate the matrices.

Capsicumicine shifts the molecular self-assembly of artificial matrices. To confirm capsicumicine interactions with staphylococcal matrix assembly in the absence of metabolic or regulatory influences, we used an artificial matrix model based on Stewart et al. (*39*). Briefly, we monitored the real-time molecular self-assembly reaction by measuring the optical density at 600 nm (OD_{600}) as a function of time with or without capsicumicine. As a negative control, we used PA-1, a similarly sized peptide (*40, 41*). OD increases when capsicumicine is present, which shows that the molecular self-assembly process is quicker overall (Fig. 4*A*). Remarkably, the assembled matrix profiles are also visually different, with larger agglutinates in the presence of capsicumicine, although the matrices profiles for both controls are similar (Fig. 4 *C-E*).

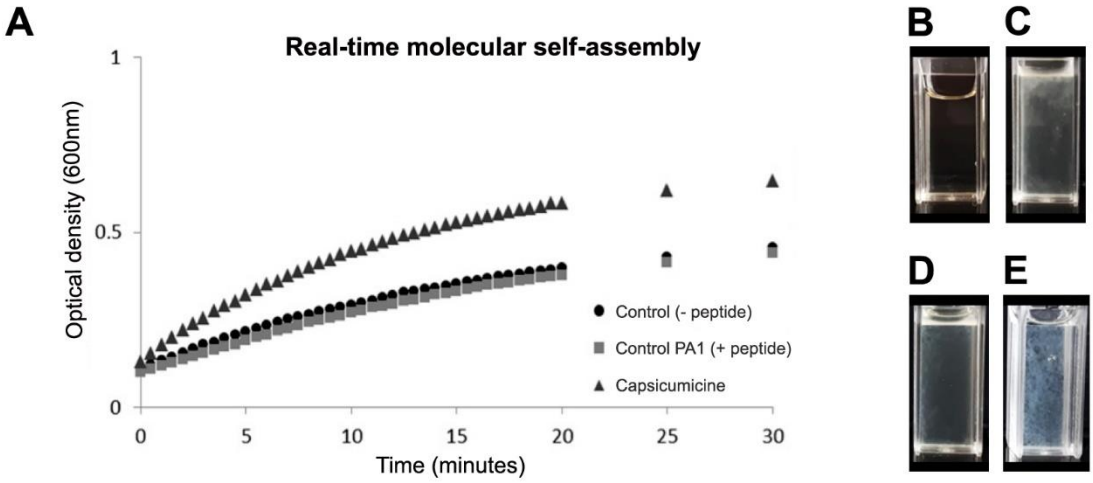

Fig. 4. Real-time molecular self-assembly (RTMSA) curves of synthetic staphylococcal matrices. (*A*) Graph of optical densities (OD_{600}) as a function of the time in minutes for the synthetic matrix in the presence of capsicumicine (triangles), the synthetic matrix positive control (circles), and the synthetic matrix PA1 peptide negative control (squares). *(B-E)* Synthetic matrix tubs in different conditions: (*B*) calibration reaction, containing all reaction compounds before polymerization; (*C*) post-polymerization positive control reaction; (*D*) post-polymerization peptide negative control reaction with PA1; and (*E*) post-polymerization capsicumicine reaction. All peptides were tested at the same final concentration.

Capsicumicine interacts with exopolysaccharides. To explore the peptide's potential affinities with these essential matrix components, we exposed *S. epidermidis* cultures to capsicumicine,

capsicumicine-FITC, and peptide antibiotic-FITC with calcofluor, then analyzed them all with CFM. We used calcofluor to target matrix polysaccharides (blue) and FITC for the peptides (green). The peptide control was an antibacterial peptide-FITC (Pseudonajide), and it showed green fluorescence in the cells but not in the matrix (Fig. 5 *E* and *F*). CFM images are shown in Fig. 5*A*, with substantial amounts of polysaccharides (blue) throughout the matrix when capsicumicine is present. Calcofluor is also seen in cells due to saccharides in the walls. Additionally, considerable amounts of capsicumicine-FITC appear exclusively on the matrix (Fig. 5*C*). To explore whether capsicumicine features are compatible with carbohydrate-binding domains (CBMs), we used chitin-, chitosan-, and PIA-binding proteins (Table S2) for capsicumicine BLAST and amino acid alignments. UniProt tools (*42*) and CAZy information crossing (*43*) showed that capsicumicine does in fact present CBM homology with all proteins tested (Fig. S2), reinforcing the idea that capsicumicine interacts with these saccharides.

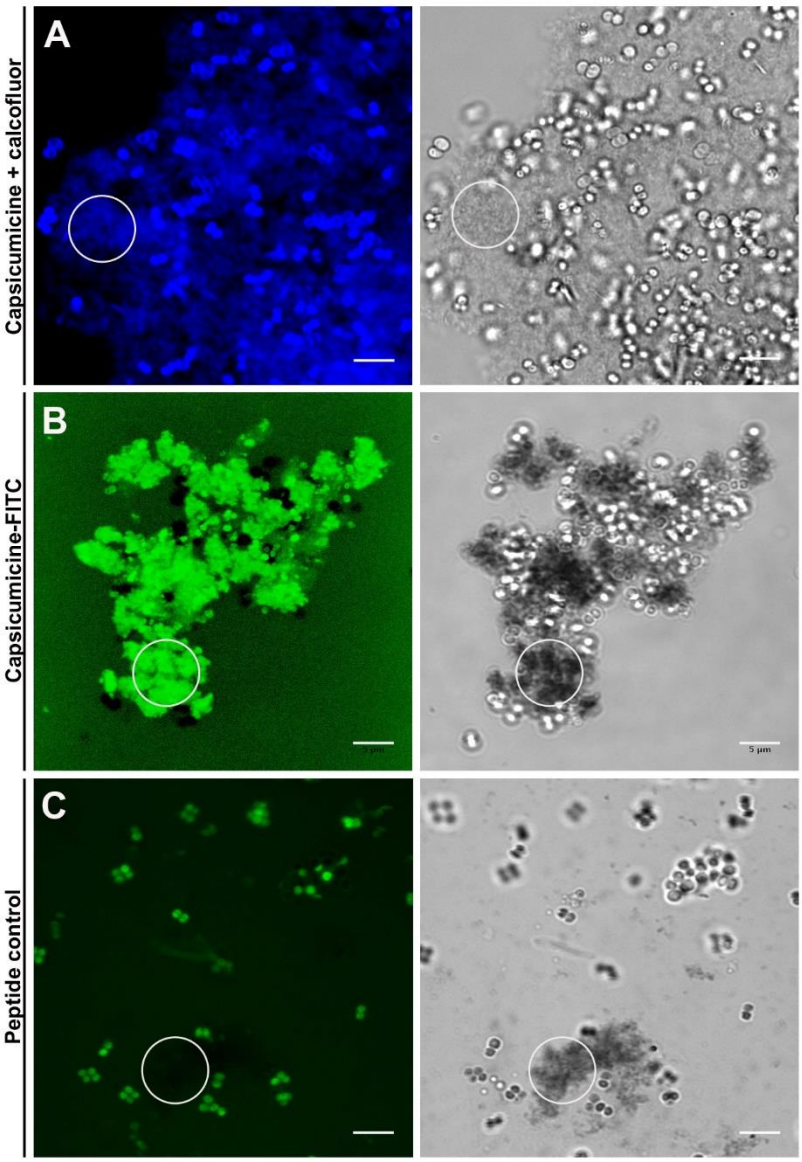

Fig. 5. Confocal fluorescence microscopy (CFM) of *Staphylococcus epidermidis* (ATCC 35984). Calcofluor was used to highlight matrix polysaccharides (blue), and FITC used for the peptides (green). Visualization was done by fluorescence (left) and transmitted light (right) microscopy. (*A*) Cultures exposed to capsicumicine and calcofluor. (*B*) Cultures exposed to capsicumicine-FITC. (*C*) Peptide negative control cultures exposed to an antimicrobial peptide-FITC (Pseudonajide). The matrix is highlighted (circles). Scale bars, 5 µm.

Discussion

Natural peptides are increasingly being explored as alternative biofilm controls, and are sure to become important allies in the fight against bacterial tolerance and resistance (*15, 44-46*). As shown here, capsicumicine, a peptide derived from *Capsicum baccatum* red pepper seeds, possesses strong antibiofilm activity. Capsicumicine prevents the establishment and maintenance of biofilm architecture through a mechanism of action that we have named "matrix anti-assembly" (MAA). MAA differs from matrix *dis*assembly (*47*) as instead of de-structuring the established matrix, it acts on the initial phase of assembly to prevent correct matrix assembly. In fact, established biofilms are harder to treat than initial biofilms, as they have very complex structures (*48, 49*), and increased structural complexity means that more energy is required for disassembly (*50*).

Bacterial surface proteins can passively interact with surfaces such as medical devices, generating an initial and reversible adhesion after electrostatic and hydrophobic interactions, Van der Waals forces, hydrodynamic forces, and so on (*51-53*). Bacteria will then require matrix production in order to remain attached after these weak interactions (*23, 54*). During this process, physicochemical interactions drive molecular and colloidal matrix self-assembly, establishing a chain of dense architecture that results in stable adhesion (Fig. 6*A*) (*39, 55, 56*). In contrast, capsicumicine interacts with the extracellular matrix and modifies the self-assembly chain, resulting in a less dense and nonfunctional matrix, and impaired biofilm formation (Fig. 6*B*).

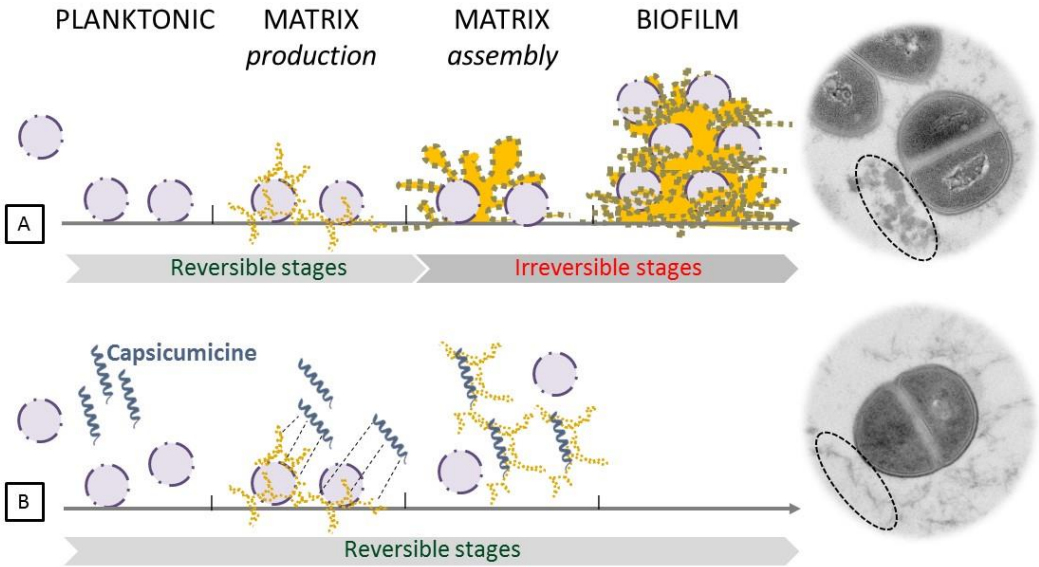

Fig. 6. Matrix anti-assembly (MAA) is a new antibiofilm mechanism of action identified in capsicumicine. This schematic highlights the formation and assembly (structuring) stages of the extracellular matrix on abiotic surfaces, with or without the peptide. (*A*) Untreated biofilm matrix development: planktonic cells interact passively with the surface and start the extracellular matrix production. Initial adhesion is established, after which matrix self-assembly occurs, leading to irreversible biofilm structuring and adhesion. As shown in the transmission electron microscopy (TEM) image (right), the extracellular matrix is densely assembled and has globular-like features. (*B*) Biofilm matrix development in the presence of capsicumicine shows the MAA. Planktonic cells are still able to interact passively with the surface to start extracellular matrix production and establish initial adhesion. At that point, capsicumicine acts as a crowding agent through physicochemical forces, attracting extracellular components such as the PIA, and shifting the self-assembly. This anti-assembly action disturbs the polymeric matrix state, reducing adhesion and aggregation, consequently the cells remain planktonic. The extracellular matrix now displays branch-like thin fibrillary oligomer structures (see TEM image). The arrows indicate reversible (green) and irreversible stages (red).

Capsicumicine's amino acid sequence suggested it has a desirable antibiofilm peptide (*15, 57*). Furthermore, it contains several residue characteristics for recognizing putative chitin-binding domains, including polar and hydrophobic residue conservation and conserved cysteine residues (*58-61*). Therefore, it displays homologies with all CBM proteins tested (Fig. S2 and Table S2). CBMs are contiguous amino acid sequences with a discreet fold, and have carbohydrate-binding activity. Among these, the chitin-binding domain is a well-conserved amino acid stretch found in plants, bacteria, and fungi, and it binds specifically to N-acetyl glucosamine, an homologous structure of PIA (*43, 62, 63*). Notably, another CBM tested, icaA, is a PIA synthetase from the same *S. epidermis* strain studied here. Capsicumicine's CBM homologies may therefore allow it to bind to saccharides.

Capsicumicine's matrix anti-assembly (MAA) mechanism of action

This proposed mechanism is based on a set of intermolecular and cooperative forces triggered by capsicumicine which then disrupt matrix assembly.

Intermolecular forces

The staphylococcal matrix is composed mainly of polysaccharides, but also contains proteins (AtlE, Aap, Empb), teichoic acids, and extracellular DNA (*64-66*). These polysaccharides are PIA/PNAG, homoglycans of beta-1,6-linked 2-amino-2-deoxy-D-glucopyranosyl residues. The matrix contains positively-charged amino groups (PNAG), as well as negative charges from O-succinylation, which confers electrical charge lability on the matrix.

The amino acids in capsicumicine are mostly neutral, with 13 glutamines (Q) and 3 serines (S). Due to Q's amide group and S's hydroxyl group, they can generate electronegative (dipole-dipole) zones. This high electronegativity suggests that capsicumicine may interact with the positive free charges (Van der Waals forces) of the PIA/PNAG polysaccharides (*23, 67*). It is certain that capsicumicine can exert polar, non-ionic forces and thus performs moderate interactions with the matrix that can alter its self-assembly, changing the organization of this saccharide polymer chain. Since strong interactions such as ionic forces may trigger unwanted effects including matrix repulsion or sequestration (*57, 67-70*), the weaker interactions of capsicumicine are ideal.

Cooperative polymerization forces

In living systems, biomolecules perform their functions in the presence of various macromolecules of different shapes and sizes, and these interactions can include cooperative polymerization forces (*71, 72*). These forces are noncovalent and non-specific physicochemical interactions, such as depletion forces and subsequent molecular crowding. They lead to bridging, aggregation, and rheological variations (*53, 55, 73*), as is observed in the presence of capsicumicine (Fig. 3 and 4), and may contribute to MAA.

Depletion forces (DFs)

In a suspension containing different molecules, DFs are the pressures exerted by small particles, which in turn cause attractive forces between the macromolecules. DFs are only expressed in crowded environments like biofilms, driving the assembly and final shape of these structures (*74*). We suppose that capsicumicine-associated DFs may coagulate in polymer solutions, aligning multiple particles and forming fibers and parallel bundles (*75, 76*), explaining the observed branch-like profile (Fig. 3 *D* and *E*) (*77*). As a result, capsicumicine probably change the matrix molecular self-assembly, resulting in flocculation (*78*).

Molecular crowding (MC)

Briefly, MC in macromolecule solutions is characterized by a decrease in accessible volume due to high macromolecule concentrations, as well as attractive and repulsive forces between them (*71, 79*). In this way, capsicumicine enhances the aggregation kinetics (Fig. 4), possibly acting as an agent of MC, decreasing entropic forces and leading to segregation (*80*). For example, a study shows that certain molecular crowders (dextran, Ficoll, PEG, and human serum albumin) that have chemical similarities with capsicumicine (hydrophilicity, linear open chains, and neutrality) modulate refolding kinetics and decrease competing aggregation and segregation (*81*).

In conclusion, the combined intermolecular and cooperative forces exerted by capsicumicine probably influence biofilm formation, disturbing matrix self-assembly at both the molecular and colloidal levels. Consequently, matrix functionality shifts, and antibiofilm activity occurs.

For all tested genes, the capsicumicine-exposed bacteria display the same fold-change profiles as the untreated planktonic ones. This indicates that capsicumicine activity is probably independent of bacterial gene modulation, with bacteria remaining in their planktonic state without pressure to express biofilm formation factors.

Importantly, non-antibiotic treatments should be less susceptible to the phenomena of resistance development than conventional antibiotics, as microorganisms have less evolutionary pressure to generate resistance when there is no biotic activity (*82-84*). And since capsicumicine has not shown cytotoxicity when tested against different representative human cell lines, it has several crucial advantages.

Although there are no antibiofilm drugs available, here we show the relevance of this novel capsicumicine peptide as a strong antibiofilm agent, preventing both biofilm establishment and maintenance without antibiotic activity. Significantly, capsicumicine decreases *S. epidermidis* adhesion and aggregation, forcing bacteria to remain planktonic and thus easier for the innate immune system

314 and traditional antibiotics to clear (*85*). In particular, we demonstrate this peptide's innovative and
315 promising matrix anti-assembly mechanism of action, which makes it less susceptible to developing
316 bacterial resistance. Non-bactericidal peptides are therefore clearly very promising for the
317 development of new antivirulence therapies and biomaterial coatings to avoid bacterial resistance and
318 tolerance (*83, 86, 87*).

319 **Materials and Methods**

320 **Peptides.** All peptides were synthesized by Biomatik and ProteoGenix at purity grades over 95% in salts
321 suitable for cell culture. For the assays, the peptides were all solubilized in ultra-pure sterile water.

322 **Bacterial strains and growth conditions.** *Staphylococcus epidermidis* ATCC 35984 was grown overnight
323 on blood agar (Thermo Scientific Oxoid PB5039A) at 37 °C. Oxoid LB agar was used for the colony-
324 forming unit (CFU) assay. The other assays were done using a bacterial suspension of 3×10^8 CFU/mL in
325 tryptone soya broth (TSB, Oxoid) or 0.9% NaCl.

326 **Biofilm formation.** At least three technical and biological replicates were done for each assay of 1, 10,
327 or 100 µM peptide concentrations. *Biofilm formation inhibition:* A protocol adapted from Trentin et al
328 (*88*) was used, with crystal violet in 96-well BD Falcon polyvinyl chloride (PVC) microtiter plates. The
329 cell-bound stains were solubilized with absolute ethanol (Sigma-Aldrich), and absorbance was
330 measured at 570 nm using a BIO-TEK PowerWave XS plate reader. The biofilm formation control
331 represents 100% of biofilm formation. *Biofilm eradication:* Biofilm was pre-formed as described above
332 for 24 h at 37 °C without treatment. Afterwards, the wells were washed to remove planktonic cells,
333 peptide solutions and controls were added, and all were incubated for 24 h. Biofilm eradication was
334 verified by evaluating the remaining content by crystal violet.

335 **Bacterial growth assays.** *Microtiter plates:* Bacterial growth was evaluated by comparing OD_{600} values
336 at the start and end of incubation in 96-well PVC microtiter plates. *Colony-forming units:* After
337 incubation at 37 °C for 24 h, CFU/mL was calculated to determine the peptide solution's bactericidal
338 effects. The untreated growth control was considered to be 100% planktonic cells. At least three
339 technical and biological replicates were performed for all assays.

340 **Microscopic analysis.** *S. epidermidis* ATCC 35984 biofilm was cultured as described above.

341 **Scanning electron microscopy (SEM):** Sterile 10x4mm polystyrene coupons were inserted into
342 bacterial cultures in the presence or absence of capsicumicine for 1, 4, and 24 h. The coupons were
343 then washed with sterile 0.9% NaCl and fixed with 2.5% glutaraldehyde, 2% paraformaldehyde, and
344 0.1 M cacodylate buffer (pH 7.2). Afterwards, they were washed with 0.1 M cacodylate buffer and 0.2
345 M sucrose, then dehydrated with increasing concentrations of ethanol. A Leica EM CPD300 was used
346 for critical point drying of the dehydrated samples. These were then sputtered with palladium in a
347 Leica EM ACE200, and analyzed with a JEOL JSM-7100F microscope with EDS and EBSD at 10 kV.

348 **Transmission electron microscopy (TEM):** All well content was carefully detached at 1, 4, and 24 h,
349 centrifuged at 10,000 g for 15 min at 4 °C, then washed with sterile 0.9% NaCl. Fixation was performed
350 at 4 °C with sodium 0.1 M cacodylate, 2% paraformaldehyde, 2.5% glutaraldehyde, and 75 mM lysine.
351 Samples were washed with 0.1 M sodium cacodylate and 0.2 M sucrose, and contrasted with 1%
352 osmium tetroxide and 1.5% potassium ferrocyanide. Dehydration was done with a gradual solution of
353 ethanol and infiltration of increasing concentrations of LR White resin (Delta Microscopies, France). LR

White resin inclusion and polymerization were then performed over 24 h at 60 °C in the absence of O_2. Thin 80 nm sections were collected onto carbon grids, and visualized at 200 kV with an FEI Tecnai Sphera microscope equipped with a Gatan 4k x 4k CCD UltraScan camera.

Confocal fluorescence microscopy (CFM): Capsicumicine-fluorescein isothiocyanate (capsicumicine-ITC, 10 µM) was used to detect the capsicumicine peptide, whose antibiofilm activity was previously verified. After incubation for 1, 4, or 24 h, the well contents were carefully detached, centrifuged at 11,000g for 2 min at 4 °C, then washed with sterile 0.9% NaCl. The suspension was visualized directly or after adding 2 mg/mL Calcofluor White dye (Fluorescent Brightener 28, Sigma-Aldrich). To find bacterial cells permeated by the peptide control, we used an FITC-labelled antimicrobial peptide (Pseudonajide, KRFKKFFMKLK-FITC). Images were acquired via resonant scanner with a Leica SP8 DMI 6000 CS confocal microscope with hybrid detector, and ImageJ software was used for image analysis.

Quantitative reverse transcription PCR (qRT-PCR): After culturing for 24 h, RNAs were isolated from planktonic controls, biofilm controls, and from total cells exposed to 10 µM capsicumicine. An Invitrogen TRIzol Max bacterial RNA isolation kit and an Ambion TURBO DNase treatment were used as per manufacturer instructions. Total RNA concentrations and purities were assessed using a Biochrom SimpliNano spectrophotometer, and PCR reactions was done to ensure the complete absence of DNA. Each qRT-PCR reaction was then subjected to previously established quantities of cDNA (10 ng) and primers (0.2 µM). Reactional volumes were calculated using SYBR Select Master Mix (Applied Biosystems), as per the manufacturer's instructions. Primers (see Table S1) were designed using the Primer3 program, then produced by Eurofins Genomics. Applied Biosystems StepOnePlus equipment and software were used. Relative transcript levels were determined by the $2^{-\Delta\Delta ct}$ method (*89*).

Real-time molecular self-assembly (RTMSA) assay: After checking the starting point (pH 7.2) of the assembly reaction for the synthetic staphylococcal matrix (*39*), we recorded the OD_{600} as a function of the time every 30 sec until 30 min. Molecular self-assembly reactions were calculated to a final volume of 4 mL, with 0.3% chitosan (medium molecular weight, 75-85% deacetylation), 0.15% bovine serum albumin, and 0.015% lambda DNA (all from Sigma) in TSB. The concentration (µM) of tested peptides was calculated for a final volume of 4 mL. Before getting the assembly reaction pH starting points, a calibration record was done using the same reactional tube containing all reagents (auto zero). Acetic acid and NaOH were used to adjust pH, and the reaction temperature was about 30 °C.

Cytotoxicity assay: Cytotoxicity assays were performed on the ImPACcell robotic platform (BIOSIT, Université de Rennes 1). Multiparameter high-content screening (HCS) and high-content analysis (HCA) were done on 7 different mammalian lines: HuH7, CaCo-2, MDA, HCT116, PC3, NCI-H727, and MCF7. The number of normal cells is presented as residual cell percentage compared to the DMSO control average.

Acknowledgments:

General: We thank Daniel Thomas for his support, and Juliana Berland for insightful comments on the manuscript. Thanks to the Microscopy Rennes Imaging Center (MRic) and CMEBA facilities. **Funding:** This study was funded by the CAPES-COFECUB program, whose institutional partners are the Brazilian Ministry of Education's CAPES (Coordenação de Aperfeiçoamento de Pessoal de Nível Superior) agency and the French Ministère de l'Europe et des Affaires Étrangères (MEAE) and Ministère de

l'Enseignement supérieur, de la Recherche et de l'Innovation (MESRI). Support was also received from the French Agence Nationale pour la Recherche and Direction Générale de l'Armement (#ANR-14-ASTR-0001). **Author contributions:** R.G.V.B, S.C.B.G, A.J.M and R.G. designed research; R.G.V.B, S.C., R.S. performed research; R.G.V.B, A.R.Z., E.G., S.C.B.G, A.J.M and R.G. analyzed data; and R.G.V.B, A.J.M and R.G. wrote the paper. **Competing interests:** R.G.V.B, S.C.B.G, A.R.Z, A.J.M and R.G. are co-authors of a patent register of capsicumicine. Application number EP19305205.7 at European Patent Office. Specific aspect of manuscript covered in patent application: its amino acid sequence and bioactivity. **Data and materials availability:** All data needed to evaluate the conclusions in the paper are present in the paper and/or the Supplementary Materials. Additional data related to this paper may be requested from the authors.

References:

1. WHO. Global action plan on antimicrobial resistance. World Health Organization (2015). Retrieved from: https://www.who.int/antimicrobial-resistance/global-action-plan/en/
2. WHO. Antimicrobial resistance. World Health Organization (2018). Retrieved from: https://www.who.int/news-room/fact-sheets/detail/antimicrobial-resistance
3. H. Ceri *et al.*, The Calgary Biofilm Device: new technology for rapid determination of antibiotic susceptibilities of bacterial biofilms. *J Clin Microbiol* **37**, 1771-1776 (1999).
4. T. C. Conibear, S. L. Collins, J. S. Webb, Role of mutation in Pseudomonas aeruginosa biofilm development. *PLoS One* **4**, e6289 (2009).
5. A. Penesyan, M. Gillings, I. T. Paulsen, Antibiotic discovery: combatting bacterial resistance in cells and in biofilm communities. *Molecules* **20**, 5286-5298 (2015).
6. H.-C. Flemming, J. Wingender, The biofilm matrix. *Nature Reviews Microbiology* **8**, 623-633 (2010).
7. A. Taglialegna *et al.*, Staphylococcal Bap Proteins Build Amyloid Scaffold Biofilm Matrices in Response to Environmental Signals. *PLoS Pathog* **12**, e1005711 (2016).
8. N. Hoiby, T. Bjarnsholt, M. Givskov, S. Molin, O. Ciofu, Antibiotic resistance of bacterial biofilms. *International Journal of Antimicrobial Agents* **35**, 322-332 (2010).
9. C. Beloin, S. Renard, J. M. Ghigo, D. Lebeaux, Novel approaches to combat bacterial biofilms. *Curr Opin Pharmacol* **18C**, 61-68 (2014).
10. D. Davies, Understanding biofilm resistance to antibacterial agents. *Nat Rev Drug Discov* **2**, 114-122 (2003).
11. K. Y. Le, M. Otto, Quorum-sensing regulation in staphylococci-an overview. *Front Microbiol* **6**, 1174 (2015).
12. A. Brauner, O. Fridman, O. Gefen, N. Q. Balaban, Distinguishing between resistance, tolerance and persistence to antibiotic treatment. *Nat Rev Microbiol* **14**, 320-330 (2016).
13. I. Levin-Reisman *et al.*, Antibiotic tolerance facilitates the evolution of resistance. *Science* **355**, 826-830 (2017).
14. V. Defraine, M. Fauvart, J. Michiels, Fighting bacterial persistence: Current and emerging anti-persister strategies and therapeutics. *Drug Resist Updat* **38**, 12-26 (2018).
15. R. G. Von Borowski, A. J. Macedo, S. C. B. Gnoatto, Peptides as a strategy against biofilm-forming microorganisms: Structure-activity relationship perspectives. *Eur J Pharm Sci* **114**, 114-137 (2017).
16. N. Strempel, J. Strehmel, J. Overhage, Potential Application of Antimicrobial Peptides in the Treatment of Bacterial Biofilm Infections. *Current Pharmaceutical Design* **21**, 67-84 (2015).
17. R. Gomes Von Borowski, S. C. B. Gnoatto, A. J. Macedo, R. Gillet, Promising Antibiofilm Activity of Peptidomimetics. *Front Microbiol* **9**, 2157 (2018).
18. C. de la Fuente-Nunez *et al.*, D-Enantiomeric Peptides that Eradicate Wild-Type and Multidrug-Resistant Biofilms and Protect against Lethal Pseudomonas aeruginosa Infections (vol 22, pg 196, 2015). *Chemistry & Biology* **22**, 1280-1282 (2015).

19. L. N. e. a. Silva, Plant Natural Products Targeting Bacterial Virulence Factors. *Chemical Reviews* **116.16**, 9162-9236 (2016).
20. K. L. Rogers, P. D. Fey, M. E. Rupp, Coagulase-negative staphylococcal infections. *Infect Dis Clin North Am* **23**, 73-98 (2009).
21. I. Uçkay *et al.*, Meticillin resistance in orthopaedic coagulase-negative staphylococcal infections. *J Hosp Infect* **79**, 248-253 (2011).
22. A. N. Neely, M. P. Maley, Survival of enterococci and staphylococci on hospital fabrics and plastic. *J Clin Microbiol* **38**, 724-726 (2000).
23. M. Otto, Staphylococcal biofilms. *Bacterial Biofilms* **322**, 207-228 (2008).
24. T. Lalani *et al.*, Prosthetic valve endocarditis due to coagulase-negative staphylococci: findings from the International Collaboration on Endocarditis Merged Database. *Eur J Clin Microbiol Infect Dis* **25**, 365-368 (2006).
25. Y. Nishizaki *et al.*, Japanese features of native valve endocarditis caused by coagulase-negative staphylococci: case reports and a literature review. *Intern Med* **52**, 567-572 (2013).
26. D. Teterycz *et al.*, Outcome of orthopedic implant infections due to different staphylococci. *Int J Infect Dis* **14**, e913-918 (2010).
27. C. L. Abad, A. Haleem, Prosthetic Joint Infections: an Update. *Curr Infect Dis Rep* **20**, 15 (2018).
28. M. Otto, Physical stress and bacterial colonization. *FEMS Microbiol Rev* **38**, 1250-1270 (2014).
29. D. G. Maki, D. M. Kluger, C. J. Crnich, The risk of bloodstream infection in adults with different intravascular devices: a systematic review of 200 published prospective studies. *Mayo Clin Proc* **81**, 1159-1171 (2006).
30. M. E. Rupp, Clinical characteristics of infections in humans due to Staphylococcus epidermidis. *Methods Mol Biol* **1106**, 1-16 (2014).
31. CDCP, Center for Disease Control and Prevention. Vital signs: central line-associated blood stream infections -United States, 2001, 2008, and 2009. *MMWR Morb Mortal Wkly Rep* **60**, 243-248 (2011).
32. K. Sieradzki, R. B. Roberts, D. Serur, J. Hargrave, A. Tomasz, Heterogeneously vancomycin-resistant Staphylococcus epidermidis strain causing recurrent peritonitis in a dialysis patient during vancomycin therapy. *J Clin Microbiol* **37**, 39-44 (1999).
33. J. Y. H. Lee *et al.*, Global spread of three multidrug-resistant lineages of Staphylococcus epidermidis. *Nat Microbiol*, (2018).
34. A. Lazaris *et al.*, Novel multiresistance cfr plasmids in linezolid-resistant methicillin-resistant Staphylococcus epidermidis and vancomycin-resistant Enterococcus faecium (VRE) from a hospital outbreak: co-location of cfr and optrA in VRE. *J Antimicrob Chemother* **72**, 3252-3257 (2017).
35. J. M. Streit, R. N. Jones, H. S. Sader, T. R. Fritsche, Assessment of pathogen occurrences and resistance profiles among infected patients in the intensive care unit: report from the SENTRY Antimicrobial Surveillance Program (North America, 2001). *Int J Antimicrob Agents* **24**, 111-118 (2004).
36. R. K. Flamm *et al.*, Linezolid Surveillance Results for the United States (LEADER Surveillance Program 2014). *Antimicrob Agents Chemother* **60**, 2273-2280 (2016).
37. R. Hope *et al.*, Non-susceptibility trends among staphylococci from bacteraemias in the UK and Ireland, 2001-06. *J Antimicrob Chemother* **62 Suppl 2**, ii65-74 (2008).
38. P. D. Fey, M. E. Olson, Current concepts in biofilm formation of Staphylococcus epidermidis. *Future Microbiol* **5**, 917-933 (2010).
39. E. J. Stewart, M. Ganesan, J. G. Younger, M. J. Solomon, Artificial biofilms establish the role of matrix interactions in staphylococcal biofilm assembly and disassembly. *Sci Rep* **5**, 13081 (2015).
40. P. Liu *et al.*, Genetic Selection of Peptide Aptamers That Interact and Inhibit Both Small Protein B and Alternative Ribosome-Rescue Factor A of Aeromonas veronii C4. *Front Microbiol* **7**, 1228 (2016).

41. P. Liu *et al.*, Targeting Inhibition of SmpB by Peptide Aptamer Attenuates the Virulence to Protect Zebrafish against. *Front Microbiol* **8**, 1766 (2017).
42. The UniProt Consortium, UniProt: the universal protein knowledgebase. *Nucleic Acids Res* **45**, D158-D169 (2017).
43. V. Lombard, H. Golaconda Ramulu, E. Drula, P. M. Coutinho, B. Henrissat, The carbohydrate-active enzymes database (CAZy) in 2013. *Nucleic Acids Res* **42**, D490-495 (2014).
44. P. S. Stewart, Prospects for Anti-Biofilm Pharmaceuticals. *Pharmaceuticals (Basel)* **8**, 504-511 (2015).
45. C. Feuillie *et al.*, Molecular interactions and inhibition of the staphylococcal biofilm-forming protein SdrC. *Proc Natl Acad Sci U S A* **114**, 3738-3743 (2017).
46. L. Grassi, G. Maisetta, S. Esin, G. Batoni, Combination Strategies to Enhance the Efficacy of Antimicrobial Peptides against Bacterial Biofilms. *Front Microbiol* **8**, 2409 (2017).
47. R. Roy, M. Tiwari, G. Donelli, V. Tiwari, Strategies for combating bacterial biofilms: A focus on anti-biofilm agents and their mechanisms of action. *Virulence* **9**, 522-554 (2018).
48. K. Lewis, Riddle of biofilm resistance. *Antimicrob Agents Chemother* **45**, 999-1007 (2001).
49. S. Jabbouri, I. Sadovskaya, Characteristics of the biofilm matrix and its role as a possible target for the detection and eradication of Staphylococcus epidermidis associated with medical implant infections. *FEMS Immunol Med Microbiol* **59**, 280-291 (2010).
50. D. Fleming, K. P. Rumbaugh, Approaches to Dispersing Medical Biofilms. *Microorganisms* **5**, (2017).
51. P. Speziale, G. Pietrocola, T. J. Foster, J. A. Geoghegan, Protein-based biofilm matrices in Staphylococci. *Front Cell Infect Microbiol* **4**, 171 (2014).
52. C. R. Armbruster, M. R. Parsek, New insight into the early stages of biofilm formation. *Proc Natl Acad Sci U S A* **115**, 4317-4319 (2018).
53. C. Even *et al.*, Recent advances in studying single bacteria and biofilm mechanics. *Adv Colloid Interface Sci* **247**, 573-588 (2017).
54. M. Otto, Staphylococcal Infections: Mechanisms of Biofilm Maturation and Detachment as Critical Determinants of Pathogenicity. *Annual Review of Medicine, Vol 64* **64**, 175-188 (2013).
55. G. Dorken, G. P. Ferguson, C. E. French, W. C. Poon, Aggregation by depletion attraction in cultures of bacteria producing exopolysaccharide. *J R Soc Interface* **9**, 3490-3502 (2012).
56. J. Schwarz-Linek *et al.*, Phase separation and rotor self-assembly in active particle suspensions. *Proc Natl Acad Sci U S A* **109**, 4052-4057 (2012).
57. A. Sharma, P. Gupta, R. Kumar, A. Bhardwaj, dPABBs: A Novel in silico Approach for Predicting and Designing Anti-biofilm Peptides. *Sci Rep* **6**, 21839 (2016).
58. T. Suetake *et al.*, Chitin-binding proteins in invertebrates and plants comprise a common chitin-binding structural motif. *J Biol Chem* **275**, 17929-17932 (2000).
59. H. Hemmi, J. Ishibashi, T. Tomie, M. Yamakawa, Structural basis for new pattern of conserved amino acid residues related to chitin-binding in the antifungal peptide from the coconut rhinoceros beetle Oryctes rhinoceros. *J Biol Chem* **278**, 22820-22827 (2003).
60. H. T. Wright, G. Sandrasegaram, C. S. Wright, Evolution of a family of N-acetylglucosamine binding proteins containing the disulfide-rich domain of wheat germ agglutinin. *J Mol Evol* **33**, 283-294 (1991).
61. J. Yin, S. Yang, K. Li, W. Guo, Y. Cao, Identification and molecular characterization of a chitin-binding protein from the beet webworm, Loxostege sticticalis L. *Int J Mol Sci* **15**, 19147-19161 (2014).
62. S. El-Gebali *et al.*, The Pfam protein families database in 2019. *Nucleic Acids Res* **47**, D427-D432 (2019).
63. W. Suginta, P. Sirimontree, N. Sritho, T. Ohnuma, T. Fukamizo, The chitin-binding domain of a GH-18 chitinase from Vibrio harveyi is crucial for chitin-chitinase interactions. *Int J Biol Macromol* **93**, 1111-1117 (2016).

64. H. Rohde, S. Frankenberger, U. Zähringer, D. Mack, Structure, function and contribution of polysaccharide intercellular adhesin (PIA) to Staphylococcus epidermidis biofilm formation and pathogenesis of biomaterial-associated infections. *Eur J Cell Biol* **89**, 103-111 (2010).
65. C. R. Arciola, D. Campoccia, P. Speziale, L. Montanaro, J. W. Costerton, Biofilm formation in Staphylococcus implant infections. A review of molecular mechanisms and implications for biofilm-resistant materials. *Biomaterials* **33**, 5967-5982 (2012).
66. A. E. Paharik, A. R. Horswill, The Staphylococcal Biofilm: Adhesins, Regulation, and Host Response. *Microbiol Spectr* **4**, (2016).
67. C. Vuong *et al.*, Polysaccharide intercellular adhesin (PIA) protects Staphylococcus epidermidis against major components of the human innate immune system. *Cell Microbiol* **6**, 269-275 (2004).
68. F. L. Brancatisano *et al.*, Inhibitory effect of the human liver-derived antimicrobial peptide hepcidin 20 on biofilms of polysaccharide intercellular adhesin (PIA)-positive and PIA-negative strains of Staphylococcus epidermidis. *Biofouling* **30**, 435-446 (2014).
69. G. Batoni, G. Maisetta, S. Esin, Antimicrobial peptides and their interaction with biofilms of medically relevant bacteria. *Biochimica Et Biophysica Acta-Biomembranes* **1858**, 1044-1060 (2016).
70. C. Chan, L. L. Burrows, C. M. Deber, Alginate as an auxiliary bacterial membrane: binding of membrane-active peptides by polysaccharides. *J Pept Res* **65**, 343-351 (2005).
71. S. F. Banani, H. O. Lee, A. A. Hyman, M. K. Rosen, Biomolecular condensates: organizers of cellular biochemistry. *Nat Rev Mol Cell Biol* **18**, 285-298 (2017).
72. C. Rest, R. Kandanelli, G. Fernández, Strategies to create hierarchical self-assembled structures via cooperative non-covalent interactions. *Chem Soc Rev* **44**, 2543-2572 (2015).
73. A. Kudlay, M. S. Cheung, D. Thirumalai, Influence of the shape of crowding particles on the structural transitions in a polymer. *J Phys Chem B* **116**, 8513-8522 (2012).
74. D. Marenduzzo, K. Finan, P. R. Cook, The depletion attraction: an underappreciated force driving cellular organization. *J Cell Biol* **175**, 681-686 (2006).
75. H. X. Zhou, Effect of mixed macromolecular crowding agents on protein folding. *Proteins* **72**, 1109-1113 (2008).
76. E. P. O'Brien, J. E. Straub, B. R. Brooks, D. Thirumalai, Influence of Nanoparticle Size and Shape on Oligomer Formation of an Amyloidogenic Peptide. *J Phys Chem Lett* **2**, 1171-1177 (2011).
77. A. Sakaguchi, K. Higashiguchi, K. Matsuda, Bundle formation of supramolecular fibers of amphiphilic diarylethene by depletion force. *Chem Commun (Camb)* **54**, 4298-4301 (2018).
78. R. Fantoni, A. Santos, Depletion force in the infinite-dilution limit in a solvent of nonadditive hard spheres. *J Chem Phys* **140**, 244513 (2014).
79. W. M. Aumiller, B. W. Davis, C. D. Keating, Phase separation as a possible means of nuclear compartmentalization. *Int Rev Cell Mol Biol* **307**, 109-149 (2014).
80. J. M. Polson, D. R. Kerry, Segregation of polymers under cylindrical confinement: effects of polymer topology and crowding. *Soft Matter* **14**, 6360-6373 (2018).
81. S. Biswas, J. Kundu, S. K. Mukherjee, P. K. Chowdhury, Mixed Macromolecular Crowding: A Protein and Solvent Perspective. *ACS Omega* **3**, 4316-4330 (2018).
82. D. A. Rasko, V. Sperandio, Anti-virulence strategies to combat bacteria-mediated disease. *Nat Rev Drug Discov* **9**, 117-128 (2010).
83. A. M. Krachler, K. Orth, Targeting the bacteria-host interface: strategies in anti-adhesion therapy. *Virulence* **4**, 284-294 (2013).
84. L. Travier, O. Rendueles, L. Ferrieres, J.-M. Herry, J.-M. Ghigo, Escherichia coli Resistance to Nonbiocidal Antibiofilm Polysaccharides Is Rare and Mediated by Multiple Mutations Leading to Surface Physicochemical Modifications. *Antimicrobial Agents and Chemotherapy* **57**, 3960-3968 (2013).

85. C. de la Fuente-Núñez, F. Reffuveille, L. Fernández, R. E. Hancock, Bacterial biofilm development as a multicellular adaptation: antibiotic resistance and new therapeutic strategies. *Curr Opin Microbiol* **16**, 580-589 (2013).
86. S. H. Mandava, E. C. Serefoglu, M. T. Freier, S. K. Wilson, W. J. Hellstrom, Infection retardant coated inflatable penile prostheses decrease the incidence of infection: a systematic review and meta-analysis. *J Urol* **188**, 1855-1860 (2012).
87. G. D. Wright, Antibiotic Adjuvants: Rescuing Antibiotics from Resistance. *Trends in Microbiology* **24**, 862-871 (2016).
88. D. S. Trentin *et al.*, Natural Green Coating Inhibits Adhesion of Clinically Important Bacteria. *Scientific Reports* **5**, (2015).
89. K. J. Livak, T. D. Schmittgen, Analysis of relative gene expression data using real-time quantitative PCR and the 2(-Delta Delta C(T)) Method. *Methods* **25**, 402-408 (2001).

Supplementary Materials

Table S1. Primers used in this study. These were previously designed using the Primer3 program, and standardized by our team.

Gene	Forward primer 5'-3'	Reverse primer 5'-3'	Amplicon
atlE	TACCAGGGTTTGCAGGATTC	GGCGCTAAATTCATTGGAAA	85 pb
aap	AGGCCGTACCAACAGTGAAT	ATGGGCAAACGTAGACAAGG	100 pb
agrC	TCATCAATATCGCATTCATCG	CCTAAACCGCGATTATCACC	136 pb
icaA	TTATCAATGCCGCAGTTGTC	CCGTTGGATATTGCCTCTGT	104 pb
leuA	GATGATCTCGGAATGGCAGT	TGAGGCATTTCCTGCTCTTT	108 pb
saeR	GCTAACACTGTCAATGTCCACA	AGGCCCCACACAGTTGTAAT	92 pb
saeS	GGCGTCAATTTGTTGTGCTA	AGGGCATAGGTATCGTTCCA	140 pb
sarA	TTTGCTTCTGTGATACGGTTGT	CGTAATGAACACGATGAAAGAACT	107 pb
gyrB	ATCAACATCGGCATCAGTCA	GCATTTGGTACGGGTATTGG	87 pb
rrsA	AAGCAACGCGAAGAACCTTA	ATGCACCACCTGTCACTCTG	95 pb

Table S2. Carbohydrate-binding domain proteins that are capsicumicine homologs. These proteins are available in the UniProtKB database and were used for BLAST and amino acid alignments to perform similarity analysis.

Entry	Name	Accession ID

ICAA_STAEQ	Intercellular adhesion protein icaA	Q5HKQ0.1
ICAD_STAEQ	Poly-beta-1,6-N-acetyl-D-glucos. synthase prot. icaD	Q5HKP9
A7Z8H9_BACVZ	Chitosanase	A7Z8H9
A0A0N0MLT5_9ACTN	Chitosanase	A0A0N0MLT5
CBP2_MOROL	Chitin-binding protein 2	C0HKC5
A0A1R0GTZ5_9FUNG	Chitin synthase 8	A0A1R0GTZ5
A0A194V113_9PEZI	Chitin biosynthesis protein CHS5	A0A194V113

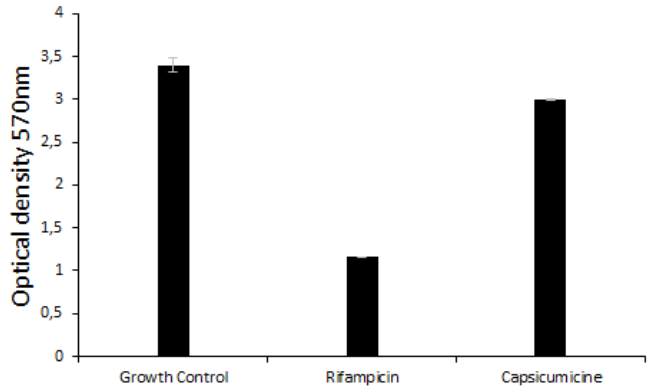

Fig. S1. Biofilm eradication test. Shown are *Staphylococcus epidermidis* (ATCC 35984) biofilm quantifications at OD_{570} for the bacterial biofilm without peptide exposure ("Growth Control"), after exposure to the rifampicin antibiotic control, and after 24 h treatment with 100 µM capsicumicine.

Fig. S2. Amino acid alignment of capsicumicine and its carbohydrate-binding domain protein homologs. (*a*) The icaA (protein accession number Q5HKQ0.1) fragment from 1 to 60. (*b*) Capsicumicine fragment from 1 to 21. (*c*) Chitosanase (A7Z8H9) fragment from 1 to 60 and from 61 to 120. (*d*) Capsicumicine fragment from 1 to 15 and from 16 to 22. (*e*) Chitin synthase 8 (A0A1R0GTZ5) fragment from 1801 to 1860 and from 1921 to 1967. (*f*) Capsicumicine fragment from 1 to 14 and from 16 to 22. Equal (* and grey highlighting), similar (.), and highly similar (:) amino acids are indicated, as well as amino acid polar characteristics (purple). Support for this analysis is available at UniProt.

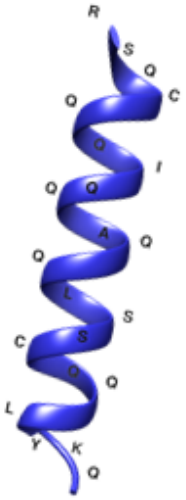

Fig. S3. Predicted capsicumicine structure. It is highly probable that this peptide has a helical conformation with a small disorganized terminal portion. The predicted structure shown here was produced using the PEP-FOLD3 computational framework (http://bioserv.rpbs.univ-paris-diderot.fr/services/PEP-FOLD3).